Atmospheric Research 290 (2023) 106794

Contents lists available at ScienceDirect

Atmospheric Research

journal homepage: www.elsevier.com/locate/atmosres

Invited review article

Assessment of HARMONIE-AROME in the simulation of the convective activity associated to a subtropical transition using satellite data

C. Calvo-Sancho [a], L. Quitián-Hernández [a], P. Bolgiani [b], J.J. González-Alemán [c], D. Santos-Muñoz [d], M.L. Martín [a,e,*]

[a] Department of Applied Mathematics, Faculty of Computer Engineering, University of Valladolid, Segovia, Spain
[b] Department of Earth Physics and Astrophysics, Faculty of Physics, Complutense University of Madrid, Madrid, Spain
[c] Agencia Estatal de Meteorología (AEMET), Department of Development and Applications, Madrid, Spain
[d] Danmarks Meteorologiske Institut. Denmark
[e] Institute of Interdisciplinary Mathematics (IMI), Complutense University of Madrid, Madrid, Spain.

ARTICLE INFO

Keywords:
Subtropical transition
Spatial verification
SAL object-based method
FSS objective-robust neighborhood verification technique
HARMONIE-AROME

ABSTRACT

Subtropical transition events (STT) are a challenge for forecasting and research due to the hybrid characteristics they give to the cyclones. The ability and skillfulness of the HARMONIE-AROME model to reproduce the cloud structure and convection associated to the October 2014 STT is here evaluated. Brightness temperature, cloud top height and accumulated precipitation are assessed against satellite data using traditional skill scores and object-based techniques specific to forecasting spatial evaluation. The results present differences in the simulation of the cyclone between the periods before and after the transition. They also show a very good performance of the model in the location of the events and a good simulation of the intensity of the variables. The performance is sub-optimal for the estimation of the sizes of the convective objects. Brightness temperature and cloud top heights yield very good results in general, with a slight overestimation in both cases. However, the model struggles to capture the accumulated precipitation. There is scarce work evaluating the HARMONIE-AROME model in this type of events; nevertheless, the results are in line with those produced by the simulations with other numerical models. The overall performance of the model is very adequate, although it might be hindered by the internal stability of the model produced by the deep-convection computation.

1. Introduction

A cyclone transition is a process in which a tropical or extratropical cyclone has a gradual dynamic and thermodynamic transformation to a different type of cyclone. This process is evident in the cyclone's core dynamics and its frontal characteristics (Garde et al., 2010). The concept of transition appreciates that there are no physical constraints in the free atmosphere to prevent a given type of cyclone from converting into a different type or from having hybrid characteristics (Garde et al., 2010; González Alemán, 2018). There are mainly two types of cyclone transitions: extratropical transition (ET) and tropical transition (TT). An ET (Jones et al., 2003; Evans et al., 2017) is a process by which a tropical cyclone loses its warm-core and symmetric nature and gradually acquires the characteristics typical of cold-core asymmetrical cyclones. A tropical transition (TT) is the process whereby a baroclinic, high-to-moderate vertical wind shear, extratropical or subtropical cyclone is transformed into a warm-core, low vertical wind shear, tropical cyclone (Davis and Bosart, 2003, 2004). A TT process occurs when extratropical precursors associated with an upper-tropospheric disturbance or a baroclinic cyclone (among other possible disturbances), develops into a tropical cyclone (Galarneau et al., 2015).

Some systems can hold hybrid characteristics, with tropical and extratropical features (Evans and Guishard, 2009), evolving in a "never-ending TT process" which does not produce a pure type of cyclone. Within this kind of systems, the subtropical cyclones (STC) are still considered a challenge for meteorological forecasters and researchers due to their complex dynamics and rapid intensification process. Consequently, their impacts are quite harmful, similar to those caused by a tropical storm or even a hurricane (Evans and Guishard, 2009; Wang and Wu, 2004). STCs are low pressure systems with both tropical and extratropical characteristics that develop with relatively shallow-weak baroclinicity in juxtaposition with diabatic processes (Hart,

* Corresponding author at: Department of Applied Mathematics, Faculty of Computer Engineering, University of Valladolid, Segovia, Spain.
E-mail address: mlmartin@uva.es (M.L. Martín).

https://doi.org/10.1016/j.atmosres.2023.106794
Received 10 February 2023; Received in revised form 21 April 2023; Accepted 2 May 2023
Available online 3 May 2023

2003; Evans and Guishard, 2009; Davis, 2010). They have hybrid thermal structures which can mainly be described by cold upper-tropospheric and warm lower-tropospheric thermal anomalies. Therefore, a cyclone becomes a STC when its fronts are partially vanished, the convection around the surface low increases and the system shares thermodynamic structures. STCs have been observed during the early stages of hurricanes or tropical storms that, in some cases, were part of a TT process (Davis and Bosart, 2004). For instance, hurricanes Delta (2005), and Leslie (2018) acquired a subtropical nature at some point during their TT (Beven et al., 2008; Steward, 2018). The object of the current survey is a STC emerged from an extratropical cyclone that had earlier developed from a large Rossby wave. Subsequently, the cyclone experienced a low cut-off process and later isolation (Quitián-Hernández et al., 2016). Since the STC did not evolve into a tropical cyclone, it just went through what is known as a subtropical transition (STT).

Studies focusing on STT events have been carried out in different parts of the globe. STC Anita, which almost acquired hurricane category, was evaluated in the South Atlantic Ocean (Dias Pinto et al., 2013). In the North Atlantic Ocean, González-Alemán et al. (2015) analyzed hurricanes Vince and Delta which were identified as STCs in their early stages. In addition, due to their particular characteristics, there has been an increase in the number of studies concerning STTs, which has led to the development of numerous STC climatologies (Cavicchia et al., 2019; Evans and Guishard, 2009; Evans and Braun, 2012; González-Alemán et al., 2015; González-Alemán et al., 2018). In fact, due to the substantial relation between the STC strength and the diabatic processes developed by these systems over the ocean (Evans and Guishard, 2009; González-Alemán et al., 2015), and considering the importance of climate change, there is a growing interest concerning the northward deviation of their trajectories and possible impacts over western Europe (González-Alemán et al., 2018).

This paper analyzes the convection associated to a STT event occurred in October 2014. The system evolved from October 17th to October 22nd, with the transition time around 06:00 UTC on October 20th. The event made landfall on the Canary Islands, causing widespread economic and social damage mainly due to strong winds and intense precipitation. Most of the impacts affected the metropolitan area of Santa Cruz de Tenerife, with at least one deceased person, numerous floodings, landslides, flight cancellations, and fires provoked by electrical storms around the island. Quitián-Hernández et al. (2016) performed a synoptic and mesoscale analysis of this event which was finally included in the STC climatology of the Eastern North Atlantic (ENA) created by González-Alemán et al. (2015). In Quitián-Hernández et al. (2021), the same event was analyzed by means of two high-resolution numerical weather prediction (NWP) models, the Weather Research and Forecasting (WRF) and the HARMONIE-AROME model, being this the first time the later was used to simulate a STT event. A local validation through several observations (airports METAR and soundings) was carried out. As a first approach to the use of satellite data, the brightness temperature (BT) product was evaluated from a visual point of view and on average using a set of traditional skill scores.

In the current study, the analysis of the October 2014 STT event is extended to perform a more complete validation of the HARMONIE-AROME ability and effectiveness in simulating STTs events from a spatial perspective. To this end, several satellite data (BT, cloud top height and precipitation) are spatially compared to the model simulations. The study is divided into two specific periods: the pre-STT period, when the cyclone is purely extratropical, and the post-STT period, when the cyclone acquires subtropical characteristics. The satellite datasets are spatially compared to the HARMONIE-AROME results, validating the simulations through several skill scores spatially calculated to give a general idea of the model's ability. Furthermore, object-oriented metrics are also used to evaluate the model skill.

This paper is organized as follows: datasets and methodology are presented in Section 2. Section 3 includes the results and discussion of the spatial validation. Finally, the major conclusions are summarized in Section 4.

2. Data and methodology

2.1. Numerical weather prediction model

Several simulations of the October 2014 STT event are carried out using the HARMONIE-AROME model (Bengtsson et al., 2017). This is a limited-area high-resolution convection-permitting model, which uses a non-hydrostatic spectral dynamical core with a semi-Lagrangian and semi-implicit discretization of the equations. The initial and boundary conditions are obtained from the ECMWF Integrated Forecasting System (IFS) analysis of the National Meteorological Archival and Retrieval System (MARS) with a T1279 spectral solution every 6 h.

The model HARMONIE-AROME configuration (cycle v40h1.1.1) is similar to the one used by Quitián-Hernández et al. (2021) with a single domain of 2.5 km grid resolution and 65 hybrid sigma-pressure levels. The set of physics parameterization schemes used is the same as the AROME-France model (Seity et al., 2011). The most remarkable are: For shortwave radiation, the Morcrette scheme (Seity et al., 2011; Bengtsson et al., 2017). Most of the ICE-3 package (Lascaux et al., 2006) is applied for microphysics. The surface parameterization is the SURFEX scheme (Masson et al., 2013), which is composed of several physical models of land surface, cities, and lakes. For shallow convection parametrization, the EDMFm scheme is applied (de Rooy, 2014; Bengtsson et al., 2017), which uses a dual flow-mass approach capable of distinguishing both, a dry and wet updrafts. Finally, for turbulence parameterization, the HARATU scheme (Bengtsson et al., 2017) is used. The simulation is performed for 120 h, with a temporal output of 3 h, allowing a spin-up time of 12 h. It is then dived into pre-STT, 10 time-steps from 19th at 0000 UTC to 20th at 0600 UTC, and post-STT, 28 time-steps from 20th at 0600 UTC to the 23rd at 1800 UTC.

2.2. Observational datasets

As cyclones usually develop over oceanic areas, atmospheric observations and measurements are often scarce. Even when instruments are in the area, the intensity of the cyclone itself can cause the equipment to become inoperative. That is the reason why satellite products become essential when evaluating model simulations, as they are sometimes the only source of observations. In this study we use three different satellite products to evaluate the ability of the HARMONIE-AROME model to simulate the deep-moist convection associated to two different stages of a STT cyclone, diagnosing the position and height of convective clouds and precipitation.

The spinning enhanced visible and infrared imager (SEVIRI) is the main instrument of the Meteosat second generation (MSG) geostationary satellites. SEVIRI provides image data in four visible and near-infrared channels and eight infrared (IR) channels (ranging from 3.9 to 13.4 μm), providing continuous precise data throughout the atmosphere. This is usually used to enhance the quality of the initial and boundary conditions for NWP models (Pasternak et al., 1994). The eight IR channels, located in the thermal region, provide cloud, land, and sea surface temperature data. With a temporal resolution of 15 min, the horizontal resolution for the standard channels is 5 km, except for the high-resolution visible channel which has a sampling distance of 1 km at the nadir.

One of the MSG-SEVIRI products used in this study to validate the HARMONIE-AROME outputs is the BT field. According to Bormann et al. (2014) and Otkin et al. (2009), the appropriate channels to identify the top cloud cover and surface temperatures are the 8.7 μm, 10.8 μm, and 12.0 μm IR channels. Moreover, the 10.8 μm and 12.0 μm IR channels are considered to be especially sensitive to the existence of clouds (Zingerle, 2005; Bormann et al., 2014; Montejo, 2016). Furthermore, according to Chevallier and Kelly (2002), all these mentioned IR

channels are particularly accurate in detecting the cloud vertical distribution and other fields, such as temperature or emissivity. Quitián-Hernández et al. (2021) and Díaz-Fernández et al. (2022) use the 10.8 μm long-wave IR channel in subtropical cyclones and mountain waves studies demonstrating its value as observational data to validate numerical simulations. According to such studies, the 10.8 μm long-wave IR channel is selected in this study as observational data.

Another satellite variable used in the validation is the cloud top height (CTH). This has been taken from the Cloud Top Temperature and Height (CTTH) product developed by the Nowcasting Satellite Application Facilities (NWC-SAF) group, led by the Spanish Meteorological Agency within the EUMETSAT. To compute the CTTH product the 6.2, 7.0, and 7.3 μm satellite radiances and the 10.8 and 12.0 μm satellite BT are needed. Furthermore, the procedure for computing the CTH will depend on the category of the cloud, i.e., low or middle-level thick clouds, upper-level thick clouds, or upper-level semi-transparent clouds (NWC-SAF, 2023).

Finally, precipitation is one of the most important effects of this type of system, so improving rainfall prediction using meteorological models is needed. The Integrated Multi-Satellite Retrievals for the Global Precipitation Mission (IMERG; Hou et al., 2014;Huffman et al., 2015; Skofronick-Jackson et al., 2017) is an algorithm developed by NASA to estimate the accumulated precipitation in most parts of the globe by combining information from the NASA satellite constellation (Tan et al., 2017). In the current study, the IMERG-F Level 3 (Version 5) product has been used to analyze the accumulated precipitation in the study area with a spatial resolution of 0.1 × 0.1° every 30 min (NASA, 2023). It must be noted that, unfortunately, there is very scarce literature about the evaluation of this variable with the HARMONIE-AROME simulations for a proper discussion, thus we will resort mainly to studies made with the WRF model.

2.3. Methodology

Several skill scores are used to evaluate the model simulations against the satellite observations. The spatial validation is assessed calculating the skill scores for each grid point of the domain, along the temporal dimension, for the period analyzed. The results are evaluated in pre-STT and post-STT periods. The skill scores used in this study consist of relative bias (hereafter BIAS), root mean square error (RMSE), and standard deviation (STD).

In addition to these, the SAL (Structure, Amplitude, Location) object-based metric is also assessed (Wernli et al., 2009). This method was developed to quantify the model accuracy on spatial distribution, intensity, and location of precipitation objects in quantitative precipitation forecasts (Ebert and McBride, 2000; Davis et al., 2006; Früh et al., 2007). It has been proven useful in the evaluation of events in Europe, by Zimmer et al. (2008) in southern Germany and Jenkner (2008) in Switzerland. Wernli et al. (2009) applied the metric to several quantitative precipitation forecast cases in the United States showing good results for the precipitation intensity and location. They also proved that SAL is usually more accurate than the traditional skill scores when evaluating severe events. Früh et al. (2007) applied SAL to evaluate the accuracy of precipitation forecasts generated by local NWPs and satellites. Crocker and Mittermaier (2013) demonstrated that SAL can show the ability of a model to resolve cloud free areas by combining the evaluation of the entire domain with the evaluation of individual objects. Therefore, the application of SAL appears to be particularly useful for the validation of the cloud distribution and, as such, it is applied here to the BT, CTH and IMERG fields.

The SAL metric is computed independently for Structure, Amplitude, and Location of the field analyzed, and the results show deviation from the observed object. The structure and amplitude values range from −2 to +2, with a null value indicating a perfect simulation. While the structure, depicted along the x-axis, describes the object's size and shape, the amplitude, depicted along the y-axis, provides information on the intensity of the field analyzed. The location values range from 0 to +2, being zero the ideal, and is presented in a color code. It quantifies the displacement of the forecasted object in relation to the observation, considering the center of mass of each. To define each object, a threshold must be defined for the variable used. In this study, the thresholds used are: For the BT, 250 K, 240 K, 230 K and 220 K. For the CTH, 5000 m, 6000 m, 7000 m and 8000 m. For the IMERG, 25 mm, 30 mm, 35 mm and 40 mm.

Finally, the Fraction Skill Score (FSS) is an objective-robust neighborhood verification technique which is less sensitive to spatial errors than traditional skill scores. The FSS measures how the forecast skill varies with spatial scale (Roberts and Lean, 2008; Roberts, 2008; Wolff et al., 2014; Sokol et al., 2022), being less sensitive to small-scale or displacement errors. It is defined as a variation of the Brier Skill Score (Brier, 1950), and it can be considered as a Mean Squared Error computed relative to a low-skill reference forecast (Roberts and Lean, 2008). This avoids the high dependency on the frequency of the event. The FSS values range from 0 to 1, with 1 denoting the most accurate performance. The score depends on the sizes of the selected squares or windows (denoted as scales in the figures) and on the threshold values that are used to calculate fractional coverage. Thus, FSS values are larger as the domain window scale increases, which implies that lower FSS values are obtained with high-resolution NWP models (Ebert, 2009). In the current paper, similar SAL thresholds are applied in FSS results.

3. Results and discussion

In this section, the BT, CTH, and IMERG fields are used to evaluate the HARMONIE-AROME simulations of the October 2014 STT event. To this end, the results of aforementioned skill scores as well as the SAL and FSS metrics are presented. For the sake of simplicity, the analysis is based in two main areas, clearly seen in Fig. 1a: the core of the cyclone, comprising from 24° W to 18° W and from 30° N to 38°N, and the associated frontal system, east of the core.

3.1. Pre-STT results

To show a general behavior of the BT field, the BT mean configuration is depicted. The analysis of the BT average results previous to the transition time of the system (Fig. 1a, d) shows that the frontal structure of the cyclone is reproduced by the model to an adequate extent, presenting a good location of the system. Nevertheless, the HARMONIE-AROME model produces an overestimation of the BT. This can be appreciated in the whole domain; however, is most notable over the cyclone core where the satellite shows a large area of 243 K and 233 K clouds, north and west of the center, which the model fails to simulate. This overestimation of BT may be partly related to the intense convective processes taking place during the system development (Zhang et al., 2007; Weisman et al., 2008; Uboldi and Trevisan, 2015). Regarding the overestimation in the surrounding areas of the cyclone, a similar warm bias is also noticed in Quitián-Hernández et al. (2021). The evaluation of the STD of BT (Fig. 1g, j) presents a very similar image for the satellite and the model, producing very low values. However, some differences can be noted in the system shape, as the model shows a less symmetrical and more scattered structure; it could be said that the model simulates a system with more extratropical characteristics.

The average of CTH for the pre-STT period (Fig. 1b, e) must be evaluated with care. The satellite results show that the product does not fully reproduce the cloudiness shown by the BT, evident in the absence of top heights for all the low-level clouds surrounding the core of the cyclone, around 273 K to 253 K (Fig. 1a). On the other hand, some noise can be seen in the CTHs, as made obvious by the 8000 m tops near the Portuguese coast. However, this is directly produced by the model and the source has not been found, nor other authors have reported anything like this. Having this been noted, the results present a behavior similar to the BT for the core of the cyclone, with the model underestimating the

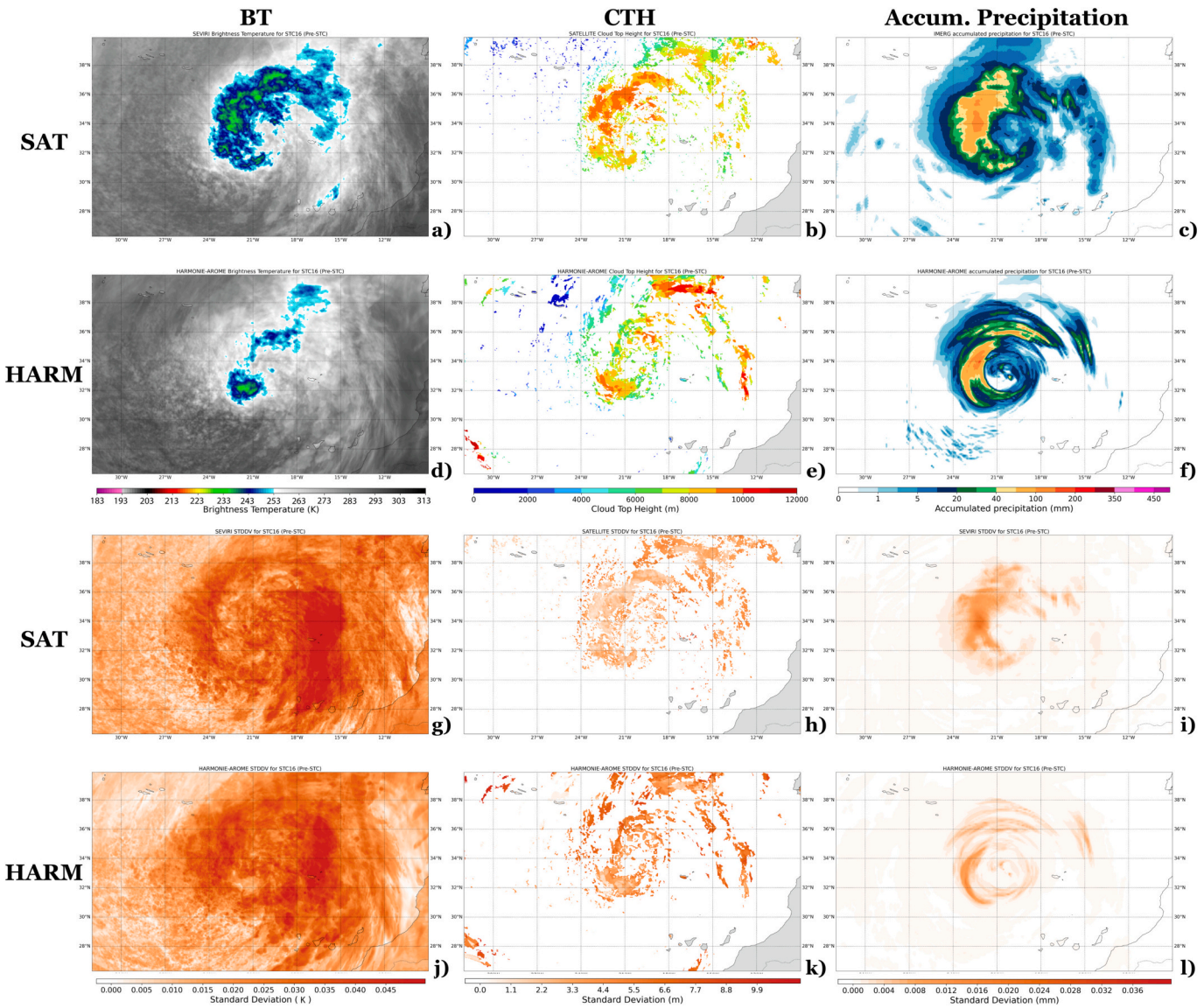

Fig. 1. a), b), c) MSG-SEVIRI mean; d), e), f) HARMONIE-AROME mean; g), h), i) MSG-SEVIRI standard deviation; j), k), l) HARMONIE-AROME standard deviation for BT (K; left column), CTH (m; center column) and accumulated precipitation (mm; right column) during the pre-STT period.

number of clouds mainly to the north and west of the center. The CTH is largely overestimated in the frontal part of the system, west of the core, presenting the model 12,000 m tops where the satellite shows 8000 and 9000 m. The STD results for the CTH (Fig. 1 h, k) are clearly higher for the HARMONIE-AROME than for the satellite. Nevertheless, the results values are low and relatively homogeneous in each domain.

The accumulated precipitation average results (Fig. 1c, f) present some underestimation by the model. As aforementioned, there is very scarce literature about the evaluation of this variable with the HARMONIE-AROME, nevertheless, these results are congruent with those of Ko et al. (2020), who used the Hurricane WRF model to simulate Hurricane Harvey. Their results showed that the model adequately reproduces the severe precipitation areas but underestimates moderate precipitation, even if the precipitation pattern of the hurricane's outer band was spatially well localized. Focusing on the core of the system, HARMONIE-AROME produces a thinner band of precipitation than the observation; it places the maximum precipitation values slightly to the east and fails to capture the precipitation to the north and north-west of the core, creating a steeper gradient of precipitation from the center to the outer system. This is congruent with the BT results. When the frontal system east of the core is evaluated, there is a large underestimation in area by the model; however, this accumulates much more precipitation than what is observed in the same area. The STD (Fig. 1i, l) presents very low values and reproduces an effect already visible in the accumulated precipitation; while the satellite depicts a diffused distribution of STD, the model shows sharper and less realistic values.

It must be noted that precipitation is a variable which still holds a large uncertainty. To the authors' knowledge, there are no studies that evaluate HARMONIE-AROME against the IMERG product. Nevertheless, there is no agreement with other limited-area high-resolution models. According to Zhang et al. (2018), precipitation results in WRF simulations are independent of the physics parameterization and grid resolution. Other studies (Pieri et al., 2015; Orr et al., 2017; Martínez-Castro et al., 2019) conclude that there is an intrinsic relation between the WRF spatial resolution or microphysics parameterization and the precipitation simulation. Even observation is subject to discussion; according to several authors (Maggioni et al., 2016; Khan et al., 2016), the accuracy of satellite-based precipitation products varies depending on the region and season observed. Some results show that IMERG typically underestimates severe precipitation during the warm seasons (Ko et al., 2020; Cui et al., 2020), while other conclude that satellite-based products exhibit high precision during the warm seasons (Zhang et al., 2018)

but tend to overestimate during the cold seasons. At the same time, model-based products yield better results in the cold seasons, as described by Khan et al. (2016) and Maggioni et al. (2016). According to these authors, the cold season evaluated in this work (October 2014) yields an excellent performance by the models against the IMERG at the reproduction of accumulated precipitation. This would be in contradiction with the results shown in Fig. 1.

Fig. 2 shows the spatial BIAS computed for the BT, CTH, and accumulated precipitation before the transition time. The results for the BT (Fig. 2a) present a large overestimation for most of the domain, with a notable underestimation where the model simulates the major cluster of clouds in the core of the cyclone. This would indicate that the model tends to generate lower clouds in general but higher clouds for deep-convection. These results agree with the average bias obtained by Quitián-Hernández et al. (2021), where fewer than observed upper-level clouds were simulated by the WRF and HARMONIE-AROME models, resulting in a larger quantity of low-level clouds. Also, the warm BIAS for the BT is supported by the computation of the spatial RMSE (not shown), which shows high RMSE values in the corresponding positive BIAS areas. Henderson et al. (2021) analyze a case study of convection initiation using three bulk cloud microphysics schemes (Morrison, Thomson and WDM6) in the WRF model obtaining negative bias in BTs associated with cloud tops. In their study, when the Morrison scheme is used, a higher fraction of convection occurs for BT near 260 K, whereas the WDM6 and Thompson schemes simulate a higher fraction of cloud tops colder than the observed by the GOES-16 imagery. Cold biases for deep convection are largest in the Morrison and Thomson schemes with the coldest bias for BTs with 240 K as more frequent value. Griffin et al. (2017) found a similar behavior when assessing output from the High-Resolution Rapid Refresh model in different convection modes. Although the HARMONIE-AROME model uses the ICE-3 scheme for microphysics, a different scheme from the Henderson et al. study, the BT show similar performance with cold bias (Fig. 2a) associated to coldest cloud tops.

The BIAS results for the CTH (Fig. 2b) also confirm what was mentioned for the average values; the model underestimates the heights to the north and west of the core, while overestimating the heights on the frontal system. In agreement with the BIAS for the BT, an overestimation of the CTH is generated for the cluster of clouds simulated in the core. The RMSE results (not shown) yield slightly higher values located to the north of the cyclone corresponding to the positive BIAS depicted in such zone (Fig. 2b), and so, to the overestimation shown in the spatial mean results (Fig. 1e). Finally, the BIAS results for the accumulated precipitation (Fig. 2c) highlight the fact that, where the model simulates clouds, the precipitation is overestimated, as seen in the average values. This is in consonance with the RMSE values (not shown).

The SAL is computed for the BT simulations by HARMONIE-AROME with four different thresholds (Fig. 3a). The structure presents relatively small but interesting variations among the thresholds. At 230 K the metric perfectly resolves the observed structure, nevertheless, this temperature threshold reduces the objects in the domain to a few spots. Every other threshold creates smaller objects ($S < 0$), in line with the underestimation of clouds already seen. The amplitude median is very close to the perfect intensity and is identical for every threshold, showing a slight underestimation ($A < 0$) of the BT. This seems to be contradictory with the aforementioned results, but it has to be considered that establishing a threshold eliminates most of the lower clouds, minimizing the effect of the warm BIAS, as the range of values is capped on one side. The location is also very accurate for most of the values ($L < 0.2$), being the 220 K threshold the worst result. Calvo-Sancho et al. (2023) produced similar SAL values for the HARMONIE-AROME and WRF assessment of four different TTs. Despite the SAL results would seem to indicate that the 230 K threshold is the best performer, when the FSS is computed (Fig. 3d), the best value is achieved by the largest scale windows and warmest BT threshold. Even more, the 250 K threshold yields better values than every other at every scale window.

When the SAL is computed for the CTH (Fig. 3b), once again the amplitude is identical for every threshold, very close to the perfect score, although this time it overestimates slightly ($A > 0$), as mentioned in the CTH average analysis. The location for this variable is even better than for the BT, however, the structure yields large variations among the thresholds. While the 5000 m CTH threshold creates larger structures, the 8000 m underestimates the size of the objects (considering the shapes shown in Fig. 1 are similar). The most accurate score is achieved by the 6000 m cut. It is worth considering that all of these are considered high clouds in this region, as per the WMO (2017), but higher tops are evaluated in consideration of the deep-moist convective processes associated with the STT events. The FSS results (Fig. 3e) give preference to the widest window and lowest CTH, achieving the best FSS score for all the pre-STT variables.

The application of the SAL metric to the accumulated precipitation (Fig. 3c) confirms that the HARMONIE-AROME performs very well on location which is almost perfect. The median amplitudes present a slight underestimation and identical values, however there is a large variation this time for each object, as evident by the vertical spread of the points. This seems to be in line with the previous results. The structure is much more concentrated for this variable, showing very similar values for every threshold this time, all of them with a slight underestimation. Wang et al. (2020) simulate heavy rainfall events associated with several landfalling tropical cyclones in China with the WRF model with data assimilation from convectional observations and IMERG rainfall products. The authors obtain FSS values around 0.45 for a 50 km scale window and 10 mm accumulated precipitation. In the current paper, no data assimilation is considered and the FSS scores (Fig. 3f) are best for the widest scale size with a FSS value of 0.53 for threshold of 25 mm and 64 km.

3.2. Post-STT results

When we evaluate the BT average results after the transition time (Fig. 4a, d) a clear improvement from the pre-STT results can be appreciated. The simulated BT field (Fig. 4d) supports the shape and

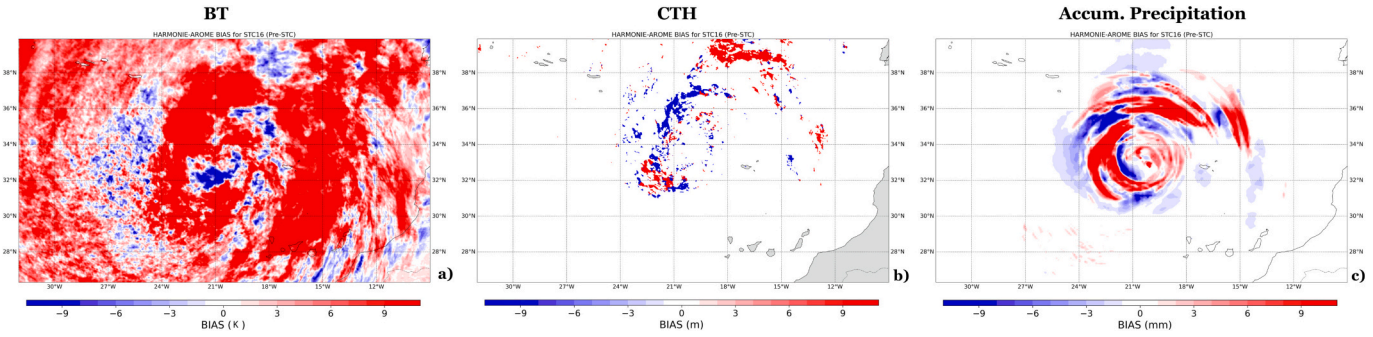

Fig. 2. HARMONIE-AROME BIAS for a) BT (k), b) CTH (m), and c) accumulated precipitation (mm) in the pre-STT period.

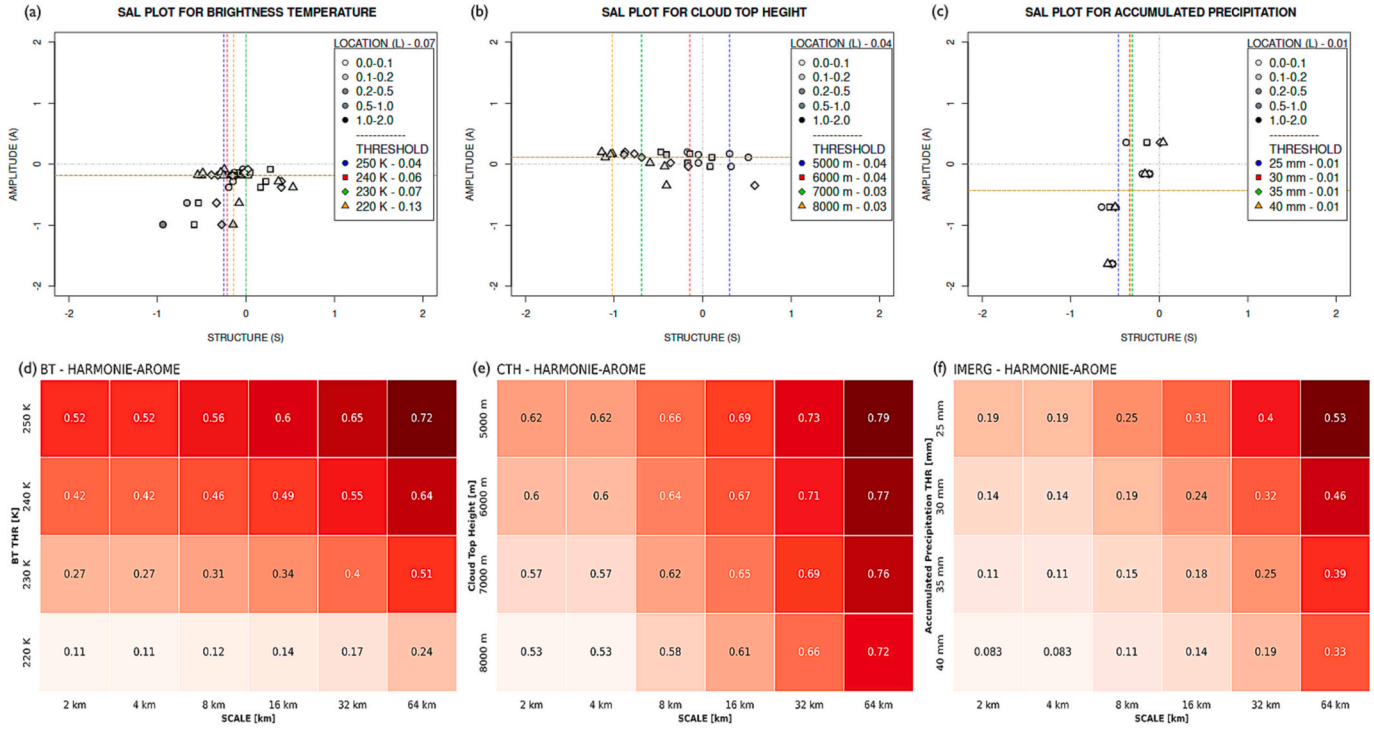

Fig. 3. SAL results for the a) BT, b) CTH, and c) accumulated precipitation during the pre-STT period. Medians for HARMONIE-AROME associated to each threshold are depicted in colored dashed lines.

location of the convective systems quite well, with values approximately 10 K higher than satellite ones. The HARMONIE-AROME is still overestimating the BT, however, to a much lower extent and with a remarkable resemblance to the satellite image in the distribution of clouds. Both the core of the cyclone and the frontal area east of it show very similar results to the satellite, as there are no "missing" clouds and the whole system is adequately simulated, albeit the mentioned overestimation of temperatures. The STD results for the BT (Fig. 4g, j) also presents very similar images for the satellite and the model. The values shown are very small and, once again, the model shows a slightly less symmetric structure than the satellite data.

The CTH results for the post-STT period (Fig. 4b, e) presents an adequate simulation of the observation, mainly at the core of the cyclone. The convective core tops are well captured by the HARMONIE-AROME model with an overestimation on the frontal areas; however, there is a large area to the north-west of the domain were the model fails to depict low clouds. The structure of the system is properly reproduced and, again, the core and frontal system do not present "missing" clouds from the observation. It must be mentioned, nevertheless, that some noise is present on the simulation of the frontal CTHs. This is more evident in the STD results (Fig. 4h, k), where higher values are shown in comparison with the satellite. The model results are also higher than the satellite in the core of the cyclone, but, overall, the results are similar and present low STD values.

In contrast with the good performance of HARMONIE-AROME simulating the BT and CTH in the post-STT period, the accumulated precipitation results (Fig. 4c, f) show a gross overestimation. While the IMERG data present the accumulated precipitation below 30 mm for most of the system and a large area of 70 mm in the southern part of the core, the model simulates the major part of the cyclone producing values over 70 mm, with an inner core ring reaching values of 200 mm. The frontal section is also overestimated in the simulation, producing values above 100 mm where the observations show precipitations below 30 mm. Nevertheless, the STD for the variable (Fig. 4i, l) presents very similar figures for the observation and model. As seen in the pre-STT, the STD values are very low and show a diffuse image for the satellite while the model creates sharper structures.

Analyzing the BIAS results for the BT in the post-STT period (Fig. 5a), the aforementioned overestimation is evident, with some areas of underestimation of the temperature of the clouds surrounding the core to the south-east and south-west. These results are also seen in the RMSE values (not shown), confirming that the HARMONIE-AROME model tends to produce lower clouds than observed, as already seen in the pre-STT period. The BIAS for the CTH (Fig. 5b) confirms the good performance of the model in this variable for the post-STT period, especially for the core of the cyclone, while the frontal system presents the overestimation of CTH already seen and in coincidence with high RMSE values (not shown). The BIAS results for the accumulated precipitation (Fig. 5c) confirm the large overestimation of the variable. Almost the whole system presents a large excess of simulated precipitation, also confirmed in the RMSE values (not shown).

The SAL results for BT on the post-STT period (Fig. 6a) present a very adequate structure and amplitude for every threshold, with a slight underestimation for both components ($A < 0$; $S < 0$), showing an improvement over the pre-STT period. The HARMONIE-AROME also shows a good performance on location, however, yields worse results for the less convective thresholds (250 K and 240 K) and maintains the same results for the highly convective ones (230 K and 220 K). Overall, the SAL values are very good for the BT, being the 250 K and 240 K thresholds the best performers. Bližňák et al. (2017) diagnose and predict the deep convective cloud and heavy rainfall evolution of some convective storms with the COSMO model using similar BT fields to this work. They obtain results indicating strong convective activity with very low BTs (210–240 K) using a threshold around 223 K. Their FSS values ($\sim$ 0.5 in average) are obtained when the scales tend to be largest and the threshold BT values tend to be lower ($\langle 220K$). In our case, the FSS values (Fig. 6d) confirm the 250 K as the best threshold with quite similar results for 240 K, producing the best score when combined with the largest scale window. Nevertheless, it must be noted that the best FSS for the post-STT is lower than the best pre-STT.

Evaluating the SAL for CTH (Fig. 6b), the same behavior is found as for the pre-STT period. The amplitude and location are identical and

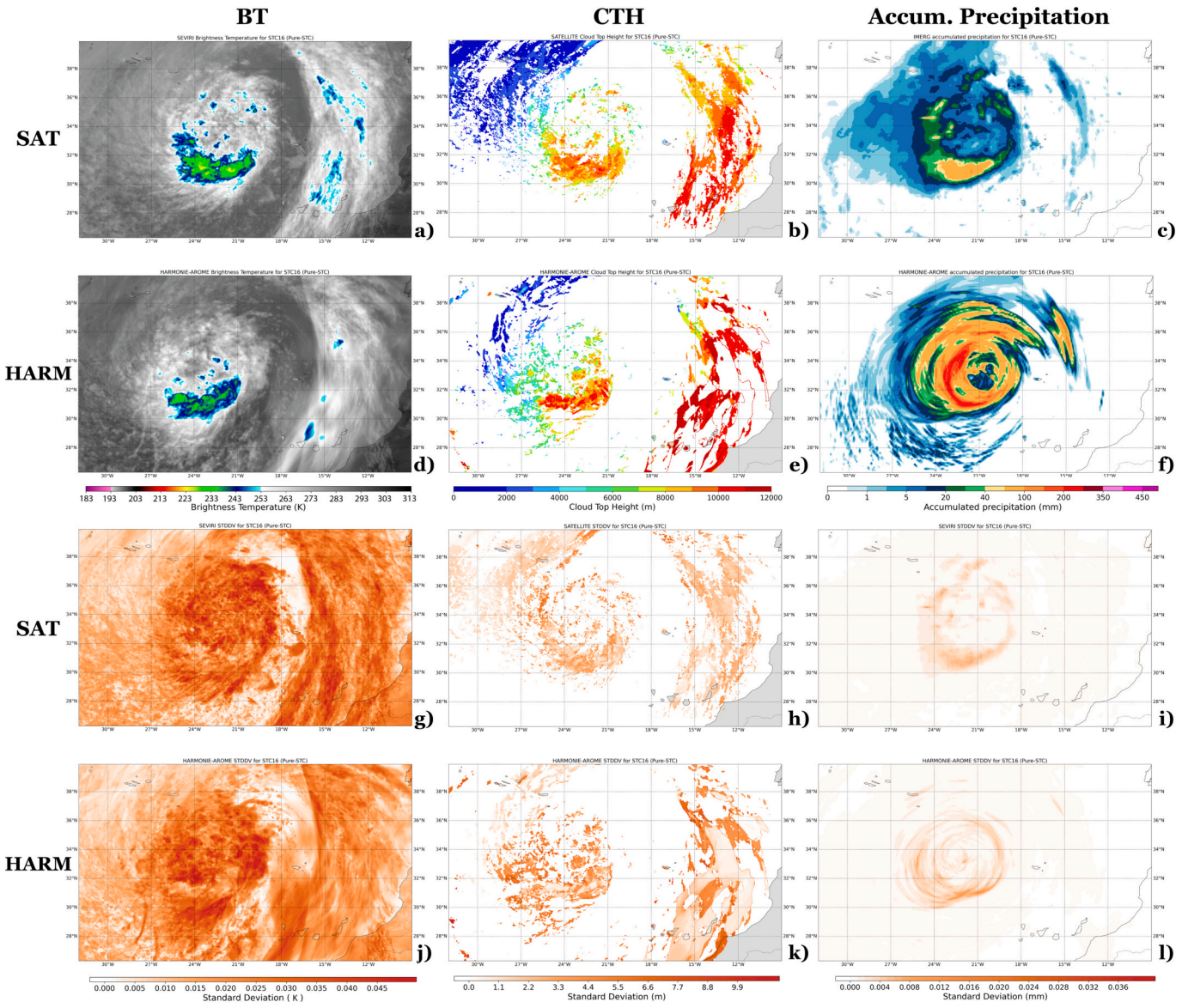

Fig. 4. Same as Fig. 1 except for the post-STT period.

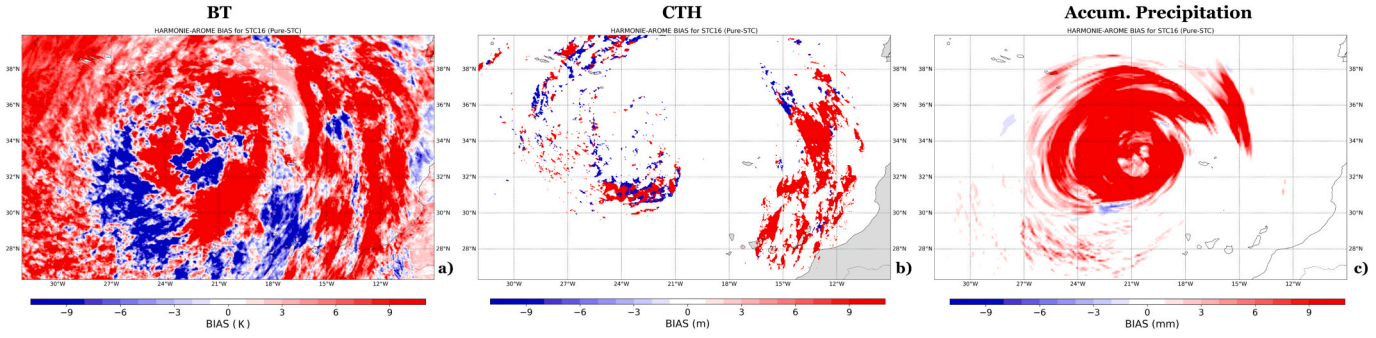

Fig. 5. Same as Fig. 2 except for the post-STT period.

very close to 0 for every threshold, with a slight overestimation on amplitude. The structure presents a smaller dispersion this period, but still showing clear differences between thresholds. As seen for the pre-STT period, the most convective threshold (8000 m) yields the worst result for structure, with a large underestimation of size, while the 5000 m threshold presents an almost perfect structure. The FSS (Fig. 6e) results confirm this threshold as the best performer, although the results are very close to those of 6000 m.

As the precipitation field usually presents more spatial variability than the cloudiness field, the scores of the simulation results are

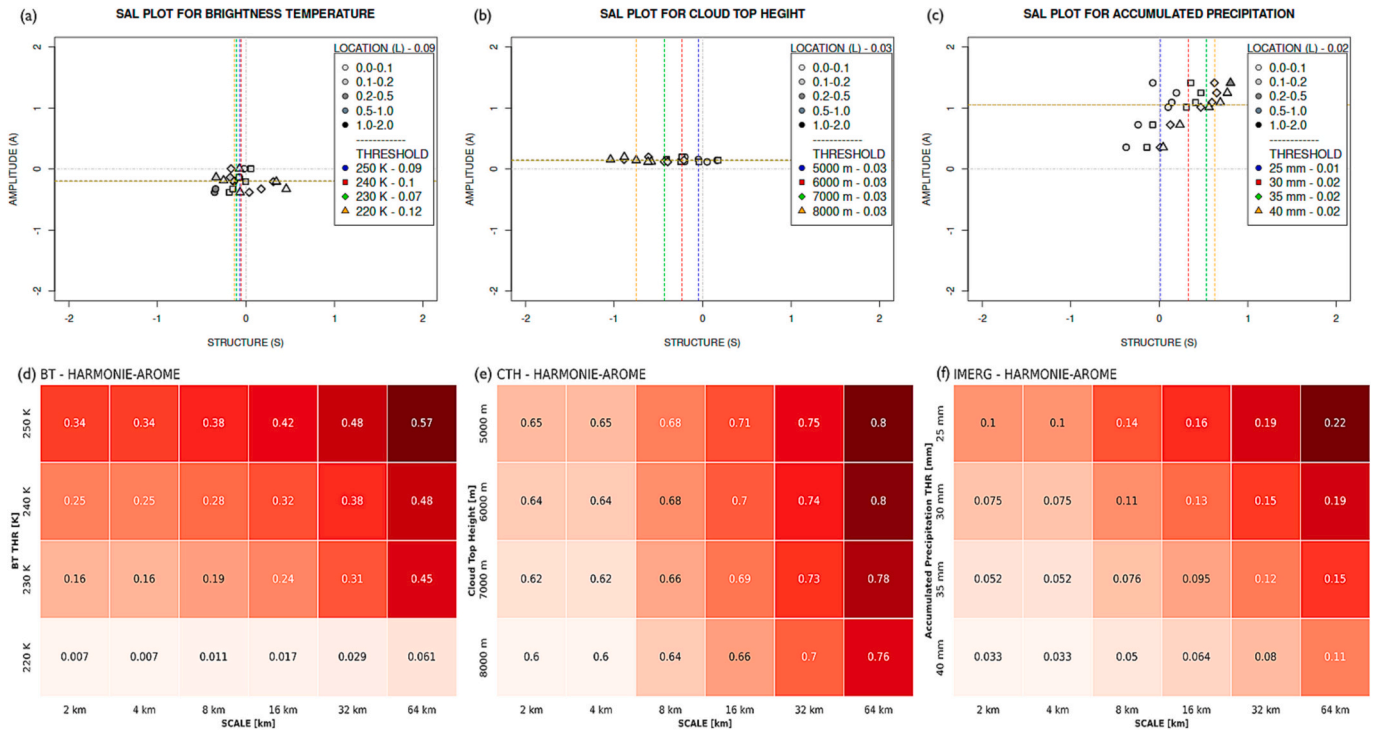

Fig. 6. Same as Fig. 3 except for the post-STT period.

certainly worse compared to those of the satellite imagery. Therefore, in contrast with the previous variables, the accumulated precipitation yields a major difference between pre-STT and post-STT. The SAL for precipitation (Fig. 6c) shows a very good performance on location, but a deterioration on structure and amplitude. The structure presents a larger dispersion between the thresholds for this period, and turns into overestimating the precipitation, although the 25 mm threshold achieves an almost perfect score. The amplitude also goes into the overestimation of the variable, as expected from previous results, presenting a lower dispersion than in the pre-STT period, but with larger medians. The FSS (Fig. 6f) clearly reflects the poor performance of the simulation with the accumulated precipitation post-STT. Bližňák et al. (2017) obtain FSS averaged values around 0.3 when using the 5 mm threshold to verify the simulated precipitation of deep convective clouds. As aforementioned, data assimilation is considered in their study, which can significantly improve forecasts from NWP models, as per Milan et al. (2008) and Sokol (2009). In our case, no data assimilation is taken into account; nevertheless, FSS around 0.22 is obtained for 25 mm, i.e., for a very strong convective activity.

4. Conclusions

The HARMONIE-AROME model is evaluated in the simulation of the convection associated to a STT occurred in October 2014 near the Canary Islands. A verification of the simulations is done at pre-STT and post-STT periods against several satellite observations, i.e., the BT observed in the 10.8 μm long-wave IR channel, the CTH derived by NWC-SAF and the accumulated precipitation IMERG data developed by NASA. The verification includes several skill scores and object-oriented metrics, spatially computed and depicted to analyze the model's ability and skillfulness when reproducing the BT, CTH and accumulated precipitation.

The results show that the convective structures are appropriately reproduced by the HARMONIE-AROME model with a good level of accuracy compared to the satellite observations. The results are clearer and more robust for the post-STT period, when the system has already undergone the transition, most probably due to the associated deep-convection during the pre-STT period.

From the BT assessment, the HARMONIE-AROME model tends to simulate smaller structures, especially at the pre-STT stage, with a very good performance on location and small errors in amplitude, denoting a generalized overestimation, most evident in the core of the cyclone during the pre-STT. These results are in accordance with Quitián-Hernández et al. (2021).

Concerning the CTH analysis, the structures are again underestimated, with a variable level of accuracy depending on the convective threshold evaluated. The dispersion is lower for the post-STT period, once again showing the influence of deep-moist convection on the model's stability. The simulation properly captures the heights, with only a small overestimation, and performs very well on the location of the cloud tops.

The accumulated precipitation results have a notable dependance on the pre-STT and post-STT stages. Also, the performance is clearly worse than the other two variables, which would be expected because of the nature of the variable and the challenge in its simulation in an extreme event like a cyclone. In general, the basic characteristics of satellite and simulated accumulated precipitation fields are similar; however, differences between the precipitation core positions are larger than in the BT simulated field. The accumulated precipitation presents an acceptable performance on amplitude for the pre-STT period, with a large overestimation during the post-STT stage. Structures tend to be smaller than observed before the transition, but larger after it, although still with an acceptable score. On the other hand, location performs very well on both periods.

Due to the difficulty of acquiring observational data in the vicinity of such an intense cyclone, it is often a challenge to validate numerical model simulations. Overall, the satisfactory results obtained from the HARMONIE-AROME model using satellite data leave the door open to the possibility of circumventing this problem and continuing to look for ways to improve the simulations. To this end, it would be very interesting to extend this study to other STTs and verification methods, and also to evaluate data assimilation. The promising results obtained in this study motivate us to further deepen the analysis of cyclones associated with tropical transition processes using high-resolution numerical

models.

Declaration of Competing Interest

The authors declare that they have no known competing financial interests or personal relationships that could have appeared to influence the work reported in this paper.

Data availability

Data will be made available on request.

Acknowledgments

This work was partially supported by research project PID2019-105306RB-I00/AEI/10.13039/501100011033, and the two ECMWF Special Projects (SPESMART and SPESVALE). C. Calvo-Sancho acknowledges the grant awarded by the Spanish Ministry of Science and Innovation - FPI program (PRE2020-092343).

References

Bengtsson, L., et al., 2017. The HARMONIE–AROME model configuration in the ALADIN–HIRLAM NWP system. Mon. Weather Rev. 145, 1919–1935. https://doi.org/10.1175/MWR-D-16-0417.1.

Beven, et al., 2008. Atlantic hurricane season of 2005. Mon. Wea. Rev 139 (2008), 1109–1173.

Bližňák, V., Sokol, Z., Zacharov, P., 2017. Nowcasting of deep convective clouds and heavy precipitation: Comparison study between NWP model simulation and extrapolation. Atmos. Res. 184, 24–34.

Bormann, N., et al., 2014. Atmospheric motion vectors from model simulations. Part I: Methods and characterization as single-level estimates of wind. J. Appl. Meteorol. Climatol. 53 (1), 47–64. https://doi.org/10.1175/JAMC-D-12-0336.1.

Brier, G.W., 1950. Verification of forecasts expressed in terms of probability. Mon. Wea. Rev 78, 1–3.

Calvo-Sancho, C., Quitián-Hernández, L., González-Alemán, J.J., Bolgiani, P., Santos-Muñoz, D., Martín, M.L., 2023. Assessing the Performance of the HARMONIE-AROME and WRF-ARW Numerical Models in North Atlantic Tropical Transitions. Atmospheric Research (Under review).

Cavicchia, L., Pepler, A., Dowdy, A., Walsh, K., 2019. A physically based climatology of the occurrence and intensification of Australian East Coast lows. J. Clim. 32, 2823–2841. https://doi.org/10.1175/JCLI-D-18-0549.1.

Chevallier, F., Kelly, G., 2002. Model clouds as seen from space: comparison with geostationary imagery in the 11-mm window channel. Mon. Weather Rev. 130, 712–722.

Crocker, R., Mittermaier, M., 2013. Exploratory use of a satellite cloud mask to verify NWP models. Meteorol. Appl. 20 (2), 197–205.

Cui, W., et al., 2020. Can the GPM IMERG final Product Accurately Represent MCSs' Precipitation Characteristics over the Central and Eastern United States? J. Hydrometeorol. 21 (1), 39–57. Retrieved Oct 1, 2021, from. https://journals.ametsoc.org/view/journals/hydr/21/1/jhm-d-19-0123.1.xml. Retrieved Oct 1, 2021, from.

Davis, C.A., Bosart, L.F., 2003. Baroclinically Induced Tropical Cyclogenesis. Mon. Wea. Rev. 131, 2730–2747. https://doi.org/10.1175/1520-0493(2003)131<2730:BITC>2.0.CO;2.

Davis, C.A., Bosart, L.F., 2004. The TT problem: forecasting the tropical transition of cyclones. BAMS 85 (11), 1657–1662. https://doi.org/10.1175/BAMS-85-11-1657.

Davis, C., Brown, B., Bullock, R., 2006. Object-based verification of precipitation forecasts. Part I: Methodology and application to mesoscale rain areas. Mon. Weather Rev. 134 (7), 1772–1784.

Davis, C.A., 2010. Simulations of subtropical cyclones in a baroclinic channel model. Journal of the atmospheric sciences 67 (9), 2871–2892.

de Rooy, W., 2014. The fog above sea problem: Part 1 analysis. Joint ALADIN-HIRLAM Newsletter, No. 2, Météo-France, Centre National de Recherches Meteorologiques, Toulouse, France, pp. 9–15. http://www.umr-cnrm.fr/aladin/IMG/pdf/ah_newsletter_2_april_2014_1_.pdf.

Dias Pinto, J.R., et al., 2013. Synoptic and dynamical analysis of subtropical cyclone Anita (2010) and its potential for tropical transition over the South Atlantic Ocean. J. Geophys. Res. Atmos. 118, 10870–10883. https://doi.org/10.1002/jgrd.50830.

Díaz-Fernández, J., Bolgiani, P., Santos-Munoz, D., Quitián-Hernández, L., Sastre, M., Valero, F., Martín, M.L., 2022. Comparison of the WRF and HARMONIE models' ability for mountain wave warnings. Atmos. Res. 265, 105890.

Ebert, E.E., 2009. Neighborhood verification: a strategy for rewarding close forecasts. Weather Forecast. 24 (6), 1498–1510.

Ebert, E.E., McBride, J.L., 2000. Verification of precipitation in weather systems: Determination of systematic errors. J. Hydrol. 239 (1–4), 179–202.

Evans, J.L., Braun, A., 2012. A climatology of subtropical cyclones in the South Atlantic. J. Clim. 25, 7328–7340. https://doi.org/10.1175/JCLI-D-11-00212.1.

Evans, J.L., Guishard, M.P., 2009. Atlantic subtropical storms. Part I: Diagnostic criteria and composite analysis. Mon. Weather Rev. 137, 2065–2080. https://doi.org/10.1175/2009MWR2468.1.

Evans, C., Wood, K.M., Aberson, S.D., Archambault, H.M., Milrad, S.M., Bosart, L.F., Zhang, F., 2017. The extratropical transition of tropical cyclones. Part I: Cyclone evolution and direct impacts. Mon. Weather Rev. 145 (11), 4317–4344.

Früh, B., Bendix, J., Nauss, T., Paulat, M., Pfeiffer, A., Schipper, J.W., et al., 2007. Verification of precipitation from regional climate simulations and remote-sensing observations with respect to ground-based observations in the upper Danube catchment. Meteorol. Z. 16 (3), 275–293.

Galarneau, T.J., McTaggart-Cowan, R., Bosart, L.F., Davis, C.A., 2015. Development of North Atlantic Tropical Disturbances near Upper-Level potential Vorticity Streamers. J. Atmos. Sci. 72, 572–597. https://doi.org/10.1175/JAS-D-14-0106.1.

Garde, L.A., Pezza, A.B., Simmonds, I., Davidson, N.E., 2010. A methodology of tracking transitioning cyclones. In: IOP Conference Series: Earth and Environmental Science (11, No. 1, p. 012007). IOP Publishing.

González Alemán, J.J., 2018. Ciclones con características tropicales sobre el Atlántico nordeste y el Mediterráneo: análisis en clima presente y proyecciones de futuro (Doctoral dissertation,. Universidad Complutense de Madrid.

González-Alemán, J.J., Valero, F., Martín-León, F., Evans, J.L., 2015. Classification and synoptic analysis of subtropical cyclones within the northeastern Atlantic Ocean. J. Clim. 28, 3331–3352. https://doi.org/10.1175/JCLI-D-14-00276.1.

González-Alemán, J.J., Gaertner, M.A., Sánchez, E., Romera, R., 2018. Subtropical cyclones near-term projections from an ensemble of regional climate models over the northeastern Atlantic basin. Int. J. Climatol. 38, 454–465. https://doi.org/10.1002/joc.5383.

Griffin, S.M., Otkin, J.A., Rozoff, C.M., Sieglaff, J.M., Cronce, L.M., Alexander, C.R., 2017. Methods for comparing simulated and observed satellite infrared brightness temperatures and what do they tell us? Weather Forecast. 32 (1), 5–25.

Hart, R.E., 2003. A cyclone phase space derived from thermal wind and thermal asymmetry. Monthly Weather Rev. 131 (4), 585–616.

Henderson, D.S., Otkin, J.A., Mecikalski, J.R., 2021. Evaluating convective initiation in high-resolution numerical weather prediction models using GOES-16 infrared brightness temperatures. Mon. Weather Rev. 149 (4), 1153–1172.

Hou, A.Y., et al., 2014. The Global Precipitation Measurement Mission. Bull. Amer. Meteor. Soc. 95, 701–722. https://doi.org/10.1175/BAMS-D-13-00164.1.

Huffman, G.J., et al., 2015. NASA Global Precipitation Measurement Integrated multi-satellitE Retrievals for GPM (IMERG). Algorithm Theoretical Basis Doc., version 4.5, 30 pp. [Available online at. http://pmm.nasa.gov/sites/default/files/document_files/IMERG_ATBD_V4.5.pdf.

Jenkner, J., 2008. Stratified Verifications of Quantitative Precipitation Forecasts over Switzerland (Doctoral dissertation,. ETH Zurich.

Jones, S.C., Harr, P.A., Abraham, J., Bosart, L.F., Bowyer, P.J., Evans, J.L., et al., 2003. The extratropical transition of tropical cyclones: Forecast challenges, current understanding, and future directions. Weather Forecast. 18 (6), 1052–1092.

Khan, S., Maggioni, V., Porcacchia, L., 2016. Uncertainties associated with the IMERG multi-satellite precipitation product. In: 2016 IEEE Int. Geoscience and Remote Sensing Symp. IEEE, Beijing, China, pp. 2127–2130. https://doi.org/10.1109/IGARSS.2016.7729549.

Ko, M.-C., et al., 2020. Evaluation of Hurricane Harvey (2017) Rainfall in Deterministic and Probabilistic HWRF forecasts. Atmosphere. 11, 666. https://doi.org/10.3390/atmos11060666.

Lascaux, F., Richard, E., Pinty, J.P., 2006. Numerical simulations of three different MAP IOPs and the associated microphysical processes. Quarterly Journal of the Royal Meteorological Society 132 (619), 1907–1926.

Maggioni, V., Meyers, P.C., Robinson, M.D., 2016. A review of merged high-resolution satellite precipitation product accuracy during the Tropical Rainfall measuring Mission (TRMM) era. J. Hydrometeorol. 17, 1101–1117. https://doi.org/10.1175/JHM-D-15-0190.1.

Martínez-Castro, D., Kumar, S., Flores Rojas, J.L., Moya-Álvarez, A., Valdivia-Prado, J. M., Villalobos-Puma, E., Castillo-Velarde, C.D., Silva-Vidal, Y., 2019. The Impact of Microphysics Parameterization in the simulation of two Convective Rainfall events over the Central Andes of Peru using WRF-ARW. Atmosphere. 10 (8), 442. https://doi.org/10.3390/atmos10080442.

Masson, V., et al., 2013. The SURFEXv7.2 land and ocean surface platform for coupled or offline simulation of earth surface variables and fluxes. Geosci. Model Dev. 6 (4), 929–960. https://doi.org/10.5194/gmd-6-929-2013.

Milan, M., Venema, V., Simmer, C., 2008. Assimilation of radar and satellite data in mesoscale models: a physical initialization scheme. Meteorol. Z. 887–902.

Montejo, I.B., 2016. Sensitivity study of the cloudiness forecast of the WRF model in the western half of Cuba. Revista Cubana de Meteorología 22 (1), 66–80. https://doi.org/10.1155/2018/1381092.

NASA, 2023. https://gpm.nasa.gov/sites/default/files/document_files/IMERG_ATBD_V5.2_0.pdf.

NWC-SAF, 2023. https://www.nwcsaf.org/ctth_description.

Orr, A., Listowski, C., Couttet, M., Collier, E., Immerzeel, W., Deb, P., Bannister, D., 2017. Sensitivity of simulated summer monsoonal precipitation in Langtang Valley, Himalaya, to cloud microphysics schemes in WRF. J. Geophys. Res. Atmos. 122, 6298–6318. https://doi.org/10.1002/2016JD025801.

Otkin, J.A., Greenwald, T.J., Sieglaff, J., Huang, H.L., 2009. Validation of a large-scale simulated brightness temperature dataset using SEVIRI satellite observations. J. Appl. Meteorol. Climatol. 48 (8), 1613–1626.

Pasternak, F., et al., 1994. Spinning enhanced visible and infrared imager (SEVIRI): The new imager for Meteosat second generation. In: Space Optics 1994: Earth Observation and Astronomy, 2209. International Society for Optics and Photonics, pp. 86–94. https://doi.org/10.1117/12.185247.

Pieri, A.B., von Hardenberg, J., Parodi, A., Provenzale, A., 2015. Sensitivity of precipitation statistics to resolution, microphysics, and convective parameterization: a case study with the high-resolution WRF climate model over Europe. J. Hydrometeorol. 16 (4), 1857–1872. Retrieved Oct 12, 2021, from. https://journals.ametsoc.org/view/journals/hydr/16/4/jhm-d-14-0221_1.xml. Retrieved Oct 12, 2021, from.

Quitián-Hernández, et al., 2016. Identification of a subtropical cyclone in the proximity of the Canary Islands and its analysis by numerical modeling. Atmos. Res. 178-179, 125–137. https://doi.org/10.1016/j.atmosres.2016.03.008.

Quitián-Hernández, et al., 2021. Analysis of the October 2014 subtropical cyclone using the WRF and the HARMONIE-AROME numerical models: Assessment against observations. Atmos. Res. 260 https://doi.org/10.1016/J.ATMOSRES.2021.105697.

Roberts, N., 2008. Assessing the spatial and temporal variation in the skill of precipitation forecasts from an NWP model. Met. Apps 15, 163–169. https://doi.org/10.1002/met.57.

Roberts, N.M., Lean, H.W., 2008. Scale-selective verification of rainfall accumulations from high-resolution forecasts of convective events. Mon. Wea. Rev. 136, 78–97. https://doi.org/10.1175/2007MWR2123.1.

Seity, Y., Brousseau, P., Malardel, S., Hello, G., Bénard, P., Bouttier, F., Lac, C., Masson, V., 2011. The AROME-France convective-scale operational model. Mon. Weather Rev. 139 (3), 976–991. https://doi.org/10.1175/2010MWR3425.1.

Skofronick-Jackson, G., et al., 2017. The Global PrecipitationMeasurement (GPM) mission for science and society. Bull. Amer.Meteor. Soc. 98, 1679–1695. https://doi.org/10.1175/BAMS-D-15-00306.1.

Sokol, Z., 2009. Effects of an assimilation of radar and satellite data on a very-short range forecast of heavy convective rainfalls. Atmos. Res. 93 (1–3), 188–206.

Sokol, Z., Brožková, R., Popová, J., Bobotová, G., Švábik, F., 2022. Evaluation of ALADIN NWP model forecasts by IR10. 8 μm and WV06. 2 μm brightness temperatures measured by the geostationary satellite Meteosat Second Generation. Atmos. Res. 265, 105920.

Steward, 2018. Hurricane Ophelia (AL172017), 2018. National Hurricane Center - Tropical Cyclone Report.

Tan, B.-Z., et al., 2017. Performance of IMERG as a function of spatiotemporal scale. J. Hydrometeorol. 18, 307–319. https://doi.org/10.1175/JHM-D-16-0174.1.

Uboldi, F., Trevisan, A., 2015. Multiple-scale error growth in a convection-resolving model. Nonlin. Processes Geophys. 22, 1–13. https://doi.org/10.5194/npg-22-1-2015.

Wang, Y., Wu, C.C., 2004. Current understanding of tropical cyclone structure andintensity changes - a review. Meteorog. Atmos. Phys. 87 (4), 257–278.

Wang, J., Xu, Y., Yang, L., Wang, Q., Yuan, J., Wang, Y., 2020. Data assimilation of high-resolution satellite rainfall product improves rainfall simulation associated with landfalling tropical cyclones in the Yangtze river Delta. Remote Sens. 12 (2), 276.

Weisman, M.L., et al., 2008. Experiences with 0–36-h Explicit Convective forecasts with the WRF-ARW Model. Weather Forecast. 23 (3), 407–437.

Wernli, H., Hofmann, C., Zimmer, M., 2009. Spatial forecast verification methods intercomparison project: Application of the SAL technique. Weather Forecast. 24 (6), 1472–1484.

Wolff, J.K., Harrold, M., Fowler, T., Gotway, J.H., Nance, L., Brown, B.G., 2014. Beyond the basics: evaluating model-based precipitation forecasts using traditional, spatial, and object-based methods. Weather Forecast. 29 (6), 1451–1472.

World Meteorological Organization (WMO), 2017. International Cloud Atlas. Available online: https://cloudatlas.wmo.int/en/useful-concepts.html.

Zhang, F., Bei, N., Rotunno, R., Snyder, C., Epifanio, C.C., 2007. Mesoscale predictability of moist baroclinic waves: Convection-permitting experiments and multistage error growth dynamics. J. Atmos. Sci. 64 (10), 3579–3594.

Zhang, J., Lin, L., Bras, R., 2018. Evaluation of the Quality of Precipitation Products: a Case Study using WRF and IMERG Data over the Central United States. J. Hydrometeorol. 19, 2007–2020.

Zimmer, M., Wernli, H., Frei, C., Hagen, M., 2008. Feature-based verification of deterministic precipitation forecasts with SAL during COPS. In: Proceedings from the MAP D-PHASE Scientific meeting in Bologna, Italy, pp. 116–121.

Zingerle, C., 2005. Satellite Data in the Verification of Model Cloud forecasts: a convective case in summer 2003 seen from NOAA satellites. Hirlam Newslet. 48, 173–177.